

Article

Ore-Bearing Fluids of the Blagodatnoye Gold Deposit (Yenisei Ridge, Russia): Results of Fluid Inclusion and Isotopic Analyses

Elena Shaparenko ^{1,*}, Nadezhda Gibsher ¹, Anatoly Tomilenko ¹, Anatoly Sazonov ², Taras Bul'bak ¹, Maria Ryabukha ¹, Margarita Khomenko ¹, Sergey Silyanov ² , Natalya Nekrasova ² and Marina Petrova ¹

¹ Sobolev Institute of Geology and Mineralogy, Siberian Branch of the Russian Academy of Sciences, 630090 Novosibirsk, Russia; gibsher@igm.nsc.ru (N.G.); tomilen@igm.nsc.ru (A.T.); taras@igm.nsc.ru (T.B.); ryabukha@igm.nsc.ru (M.R.); homenko@igm.nsc.ru (M.K.); petrovama@igm.nsc.ru (M.P.)

² Department of Geology, Mineralogy and Petrography, Siberian Federal University, 660041 Krasnoyarsk, Russia; ASazonov@sfu-kras.ru (A.S.); silyanov-s@mail.ru (S.S.); nnekrasova@sfu-kras.ru (N.N.)

* Correspondence: shaparenko@igm.nsc.ru

Abstract: The Blagodatnoye deposit with 340 t gold reserves is one of the most productive mines in Russia. Modern methods of studying fluid inclusions were used to determine the properties of fluids that formed this deposit. A comprehensive study revealed that the Blagodatnoye gold deposit was formed between 120 and 350 °C and at 0.2–2.6 kbar, and from fluids with salinities ranging from 0.5 to 30 wt.% (NaCl–eq.). These fluids are: 1—water–carbon dioxide; 2—carbon dioxide–hydrocarbon; 3—highly saline aqueous. According to Raman spectroscopy and gas chromatography–mass spectrometry, ore-forming fluids contained H₂O, CO₂, hydrocarbons and oxygenated organic compounds, sulfonated, nitrogenated and halogenated compounds. Early oxidized water–carbon dioxide fluids formed barren associations of the deposit. Later reduced carbon dioxide–hydrocarbon fluids had a key role in the formation of gold-bearing quartz veins. The stable isotope data ($\delta^{34}\text{S} = 0.8$ to 21.3‰, $\delta^{13}\text{C} = -2.8$ to -20.9 ‰, $^3\text{He}/^4\text{He} = 0.14 \pm 0.3 \times 10^{-6}$) suggest the ore-forming fluids have a crustal source.

Keywords: Yenisei Ridge; Blagodatnoye deposit; gold; fluid inclusions; gas chromatography–mass spectrometry



Citation: Shaparenko, E.; Gibsher, N.; Tomilenko, A.; Sazonov, A.; Bul'bak, T.; Ryabukha, M.; Khomenko, M.; Silyanov, S.; Nekrasova, N.; Petrova, M. Ore-Bearing Fluids of the Blagodatnoye Gold Deposit (Yenisei Ridge, Russia): Results of Fluid Inclusion and Isotopic Analyses. *Minerals* **2021**, *11*, 1090. <https://doi.org/10.3390/min11101090>

Academic Editors: Nikolay A. Goryachev, Vladimir A. Makarov and Alexander V. Volkov

Received: 18 August 2021
Accepted: 30 September 2021
Published: 3 October 2021

Publisher's Note: MDPI stays neutral with regard to jurisdictional claims in published maps and institutional affiliations.



Copyright: © 2021 by the authors. Licensee MDPI, Basel, Switzerland. This article is an open access article distributed under the terms and conditions of the Creative Commons Attribution (CC BY) license (<https://creativecommons.org/licenses/by/4.0/>).

1. Introduction

The Blagodatnoye deposit is one of largest gold deposits in Russia. Gold reserves are estimated at 340 tons averaging 1.3 g/t in ore according to the data of “Polys Gold” company [1]. The deposit is attributed to orogenic gold deposits [2]. Gold deposits of this type formed at the final stages of the formation of folded and thrust mountain structures [3]. The deposit was discovered in 1967 by Krysin M. V. in the process of geological survey 1:50,000. Polus Gold started mining at the deposit in 2010 [1]. The Blagodatnoye lies 25 km away from the Olimpiadinskoe deposit (652 t) in the North–Yenisei district of the Krasnoyarsk Territory (Figure 1a). These deposits are situated within the Yenashim ore field. The field is unique in gold reserves and ranks first in metal production of Russia [4]. There are a number of works in international and Russian journals devoted to the study of gold deposits by fluid inclusions analysis. In these works, data on the temperatures, pressures and salinity of fluids are reported [5–10]. Development of Raman spectroscopy and its application to individual fluid inclusions resulted in an increased number of works in which fluid composition is discussed [6,10–19].

Recently we developed a special device that is used for gas mixture injection upon shock destruction of a sample, which in combination with a highly sensitive gas chromatography–mass spectrometer allowed obtaining original results on the composition of gas component of fluids in native gold, quartz and sulfides from gold deposits of the

Yenisei ridge [18–21]. The aim of our work is to reveal the physicochemical properties of ore-bearing fluids that formed the Blagodatnoye deposit in the Yenisei Ridge, which ranks the second in gold reserves.

2. Geological Setting

The Blagodatnoye deposit is located on the Yenisei ridge, the tectonic evolution of which was discussed by Vernikovskiy [22]. The description of the Blagodatnoye deposit is most fully considered in the works [23–25] and consists in the following provisions. The ore field of the deposit is located in the Severo-Yeniseyskiy district of the Yenisei Ridge on the southeast wing the Panimba anticlinorium bounded by the Tatarka deep fault in the west and Ishimba deep fault in the east (Figure 1a).

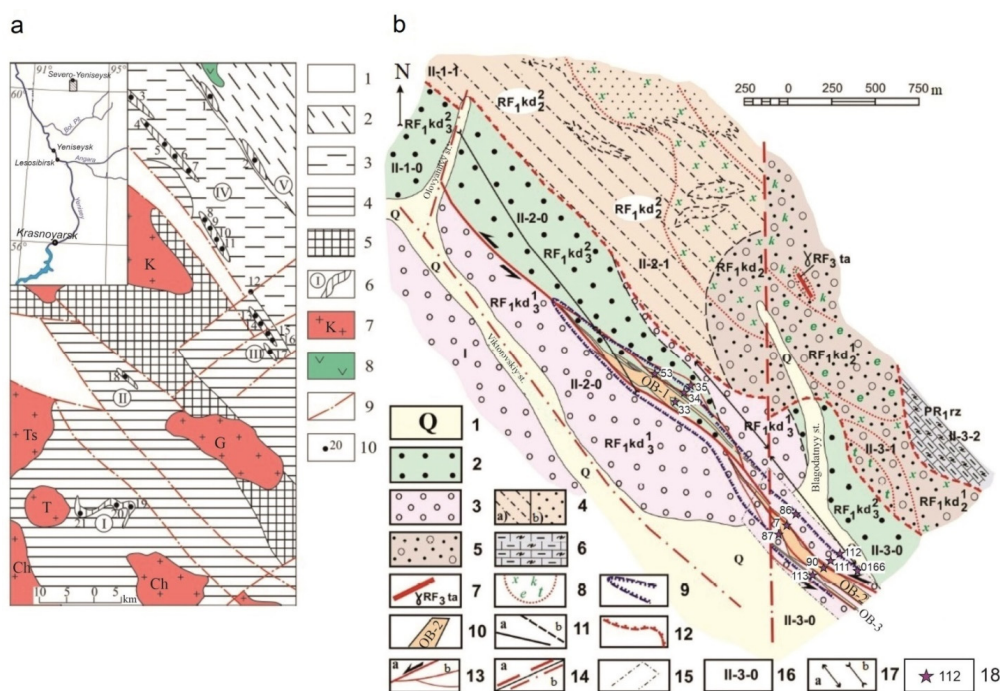


Figure 1. (a)—Geological structure of the North-Yenisei ore region [4]; (b)—Geological map of the Blagodatnoye deposit [24]. (a): 1—deposits of the Paleozoic grabens (PZ); 2—sandy-silty-clayey rocks of cata- and metagenesis zones (RF₃); 3—phyllites of the Uderey and Gorbilok formations of the Sukhoy Pit Group (RF₃); 4—crystalline schists of the biotite zone (Sukhoy Pit Group RF₁, Corda Group); 5—crystalline schists of epidote-amphibolite and amphibolite facies (Gorbilok and Corda formations; Penchenga Formation and Karpinsky Ridge Formation, Teya Group, PR₁); 6—ore zones of local dynamothermal metamorphism: I—Verkhnee Yenashimo, II—Blagodatninskaya, III—Perevalninskaya, IV—Aleksandro-Ageevskaya, V—Sovetskaya; 7—granitic plutons: K—Kalami, G—Gurakhta, T—Tyrada, Ch—Chirimba, Ts—Teya; 8—metamafic rocks, 9—disjunctive faults; 10—gold deposits: 1—Sovetskoye, 2—Ogne-Poteryayevskoye, 3—Skalistoje, 4—Sergievskoe, 5—Polyarnaya Zvezda, 6—Zayavka 14, 7—Uspenskie Zhily, 8—Buyan, 9—Ishmurat, 10—Aleksandrovo-Ageevskoye, 11—Albanskie Zhily, 12—Proletarka, 13—Vershinka, 14—Udarny, 15—Pervenets, 16—Eldorado, 17—Olginskoye, 18—Blagodatnoye, 19–20—Olimpiada (19—Eastern, 20—Western), 21—Tyrada. (b): 1—Quaternary sediments; 2—Upper section of the Corda formation. Upper bench (RF₁kd₂²). Rhythmically layered quartz-feldspar schists; 3—Upper section of the Corda formation. Bottom bench (RF₁kd₃¹). Spotted staurolite slates; 4—Middle section of the Corda formation. Upper bench (RF₁kd₂²): (a) quartzitic schists; (b) leucocratic quartzitic schists; 5—Middle section of the Corda formation. Bottom bench (R₁kd). Medium-grained arkose metaaurolites with porphyroblasts of muscovite; 6—Ryazanov formation (Pr₁rz). Calcyphyres; 7—granite-porphry dikes. Tatar-Ayakhta intrusive complex; 8—zones of metasomatically altered rocks and diaphthorites; x—(chlorite ± pyrrhotitepyrite); e—(chlorite ± actinolite ± epidote ± sulfides); k—(chlorite ± epidote ± calcite ± pyrrhotite); t—tourmaline; 9—contour of ore-bearing mineralized zone; 10—ore bodies; 11—geologic boundaries: (a) proven; (b) probable; 12—anticipated overthrusts; 13—strike-slip fault: (a) main; (b) secondary; 14—upthrusts: (a) probable; (b) hidden under overlying deposit; 15—contours of Quaternary sediments, taken from the map; 16—number of a tectonic plate of a tectonic block, 17—projections of axial lines: a—anticlines, b—synclines; 18—well and its number.

The deposit lies in the Riphean rocks of the Corda formation intruded by granitoids of the Tatarka–Ayakhta complex. The radiometric age (Rb–Sr isochrone) of granitoids is 880–752 Ma. The carbonized sericite metasomatites in the tectonic zone were formed at 571–647 °C and 6.1–8 kbar in the time interval 800–780 Ma [25]. The surrounding schists of regional metamorphism were formed at $T = 474\text{--}550$ °C and $P = 4.5\text{--}6.6$ kbar 1000–1050 million years ago. The most prolific gold-bearing sulfide mineralization occurred between 745 and 698 Ma [23–26].

The Blagodatnoye deposit consists of a steeply dipping S-shaped gold-bearing mineralized sinistral strike-slip fault zone stretching for 3800 m with the thickness of swellings up to 250 m. The depth of the zone is not outlined. The ore-bearing zones are divided into the Northern and Southern parts by submeridional upthrow (Figure 1b). In the Northern part, ore body No.1 was identified, and in the Southern part, ore bodies No.2 and No.3, which merge with each other at a depth of 120 m. The central part of the ore bodies consists mainly quartz-vein formations of nodular and bead-like forms, which are outlined along the periphery by sulfidized sericite metasomatites with quartz-carbonate veinlets.

We distinguish three stages (pre-ore, ore and post-ore) of hydrothermal mineral formation based on spatial distribution, structural setting and mineral composition. The stage of pre-ore metasomatites occurred with the formation of garnet-containing quartz-muscovite and two-mica with banded carbonization varieties. At this pre-ore gold-barren stage, early generations of pyrite and pyrrhotite were formed frequently in association with quartz, which are spatially confined to schists designated as sulfidized schists. The sulfidation is mainly confined to fractures.

The beginning of the ore stage was preceded by rather powerful tectonic shifts, which led to the formation of a series of ore-supplying cracks filled with an ore mineral association with quartz, sulfides and native gold. Damping of hydrothermal process at the quartz-ore stage is indicated by the galena-sphalerite-chalcopyrite association in which early gold underwent recrystallization and enlargement in particle size. At the ore stage, gold-bearing quartz-vein zones were formed. These zones are composed of thin (5–10 cm) quartz nodules and ptygmatite quartz veins. Thicker zones (0.5–1.5 m) are rare. The thickness of quartz-vein zones ranges from 5 to 60 m with a lateral length to 450 m and depth of 680 m. Gold-ore and sulfide mineralization preferably develops on salbands of quartz veins in schists and along cracks in quartz veins. The main ore minerals of the ore stage are arsenopyrite, pyrite and pyrrhotite, in intergrowth with which native gold occurs.

The post-ore stage of hydrothermal activity is represented by the areas of contiguous thread-like quartz-carbonate \pm fluorite veinlets widely spread within the ore-bearing zones. These accompany quartz veins and increase the overall thickness, width and depth of quartz-veined zones. The thickness of these veinlets rarely attains 1 cm, and the length, 10–20 cm.

Quartz at the deposit is represented by a translucent aggregate of gray, light gray, smoky gray and white. The color of quartz is influenced by a different amount of finely dispersed carbonaceous matter, which is concentrated in the intergranular space and in the form of inclusions inside quartz grains. Quartz of filamentary quartz-carbonate veinlets usually does not contain carbonaceous inclusions.

The morphology of native gold varies; discontinuous veinlets, separate inclusions of isometric, plate-like, drop-like and wire-like shapes are commonly localized in the microcracks of veined quartz (Figure 2). The fineness of gold ranges from 710 to 993‰. Native gold contains insignificant admixture of Cu (0.001–0.15 wt.%) and Hg (0.006–1.73 wt.%). Invisible gold was found in arsenopyrite [4].

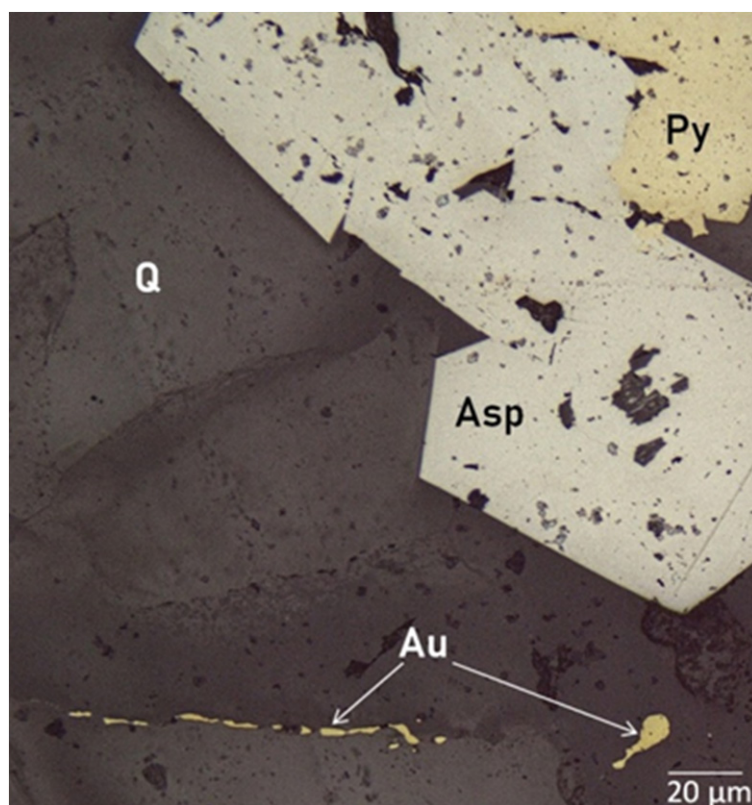


Figure 2. Native gold confined to cracks in quartz (sample 86–147.8). Q—quartz, Asp—arsenopyrite, Py—Pyrite, Au—gold.

3. Samples and Methods

In this case, 80 rock samples from the collection of prof. A.M. Sazonov were studied from 19 wells and Northern and Southern open pits of the deposit. The location of wells is shown in Figure 1b. The samples were collected from ore bodies No.1 and 2 (Figure 1b) in the range of depths from 0.6 m (well 112) to 680 m (well 0166) with a varying gold content, which ranges from 0.2 to 35.5 g/t. We used half of the sample to make doubly polished thin sections for studying individual fluid inclusions. The second half was crushed and forced through a sieve. Pure quartz, sulfides and calcite without visible impurities were picked over using a binocular magnifying glass.

The temperatures of total and partial homogenization, eutectic, ice melting, dissolution of daughter crystals and melting of liquefied gas were measured for individual inclusions. The measurements were performed in the Linkam TH–MSG–600 heating/freezing stage. The standard accuracy of measurements was ± 0.1 °C in the negative and ± 5 °C in the positive temperature range. The obtained microthermometric data allowed determination of fluid pressure according to the methods given in [27–29].

The aqueous phase composition of individual fluid inclusions was determined from the eutectic temperature, which characterizes the water–salt system [30]. The salinity of aqueous phase of inclusions was estimated from the melting point of ice and the dissolution temperature of daughter salt crystal, using the two–component water–salt NaCl–H₂O system [31] through NaCl equivalent, wt.%.

The composition of the gas phase of individual fluid inclusions in quartz was analyzed by Raman spectroscopy on Horiba J.Y. LabRAM HR800 Raman spectrometer equipped with an argon laser with a diameter of 1.5 μm and a power of 3 W, according to the method described by Dubessy [11].

The bulk composition of gas component of fluid was determined using the gas chromatography–mass spectrometry (GC-MS) on the FOCUS GC/DSQ II MS (Thermo Scientific, Waltham, MA, USA) gas chromatography–mass spectrometer. The minerals were placed in a special device connected to the gas scheme of the chromatograph in front of the analytical column. The gas mixture from fluid inclusions was extracted without pyrolysis with a single shock mechanical destruction of the sample in an inert helium flow. The purity of helium was 99.9999%. The procedure of GC-MS analysis was described in [21,32,33]. When preparing the samples for analysis, we did not use acids, solvents or organic substances which could distort the initial (parental) composition of the extracted fluid.

The sulfur isotopes ($\delta^{34}\text{S}$) of sulfides were measured in the SO_2 gas obtained during the interaction of sulfides with CuO at $1000\text{ }^\circ\text{C}$ and normalized to the isotope composition of troilite from the Canyon Diablo meteorite. The reproducibility of $\delta^{34}\text{S}$ values, including sample preparation, was 0.1% [34].

The isotope composition of helium in fluid inclusions of quartz was determined in the Laboratory of Geochronology and Geochemistry of Isotopes in the Geological Institute of the Kola Science Center of the Russian Academy of Sciences (Apatity). Methodological techniques are described in [35–39].

The isotope composition ($\delta^{13}\text{C}$) of carbon-containing compounds in fluid inclusions from quartz was determined in the gas extracted from 1000-mg samples by decrepitation with heating to $600\text{ }^\circ\text{C}$. CO_2 was bound at liquid nitrogen temperature, after which the cryo trap was isolated from the vacuum line. The ampules with CO_2 were analyzed on the ThermoFinnigan Delta Plus-XP mass spectrometer equipped with the double inlet system. The results were normalized using the VPDB (Pee Dee Belemnite) standard [10].

Isotope–geochronological data were obtained on the basis of the Ar–Ar method for determining the ages of muscovite. Muscovite from schists of quartz–muscovite–biotite \pm garnet composition in dynamothermal metamorphism zones of the Blagodatnoye deposit ore field. An installation with a quartz reactor with a fast external heating furnace was used to perform a step-heating procedure [40].

4. Results

4.1. Fluid Inclusion Types

Individual fluid inclusions were studied in quartz and calcite. Four types of fluid inclusions were found in quartz (Figure 3, Table 1):

Type A—two-phase aqueous liquid–vapor ($\text{L}_{\text{H}_2\text{O}} + \text{V}$). Liquid/vapor ratios vary from 80:20 to 20:80, respectively.

Type B—two-phase to three phase aqueous–carbonic inclusions ($\text{L}_{\text{H}_2\text{O}} + \text{L}_{\text{CO}_2} \pm \text{CH}_4 \pm \text{N}_2$, $\text{L}_{\text{H}_2\text{O}} + \text{V}_{\text{CO}_2} \pm \text{CH}_4 \pm \text{N}_2$). The ratio of water and gaseous phase also varies.

Type C—apparently single-phase liquid (or vapor) carbon dioxide–hydrocarbon ($\text{L}_{\text{CO}_2} \pm \text{CH}_4 \pm \text{N}_2$, $\text{V}_{\text{CO}_2} \pm \text{CH}_4 \pm \text{N}_2$, $\text{L}_{\text{CH}_4 + \text{N}_2}$, $\text{V}_{\text{CH}_4 + \text{N}_2} \pm \text{CO}_2$). When the temperature decreases below $0\text{ }^\circ\text{C}$, a thin rim of water solution appears in these inclusions near the walls of vacuoles.

Type D—three phase high-salinity inclusions ($\text{L}_{\text{H}_2\text{O}} + \text{V} + \text{S}$). These inclusions, in addition to aqueous and vapor phases contain solid phase (cubic crystal).

Calcite contained only one type of fluid inclusions (type A), in which the liquid phase prevails ($\text{L}_{\text{H}_2\text{O}} \gg \text{V}$).

The size of individual inclusions in the minerals under study ranges from 3 to 20 μm . Type B fluid inclusions are typically the largest, while inclusions representing post-ore stage are the smallest ($<5\text{ }\mu\text{m}$).

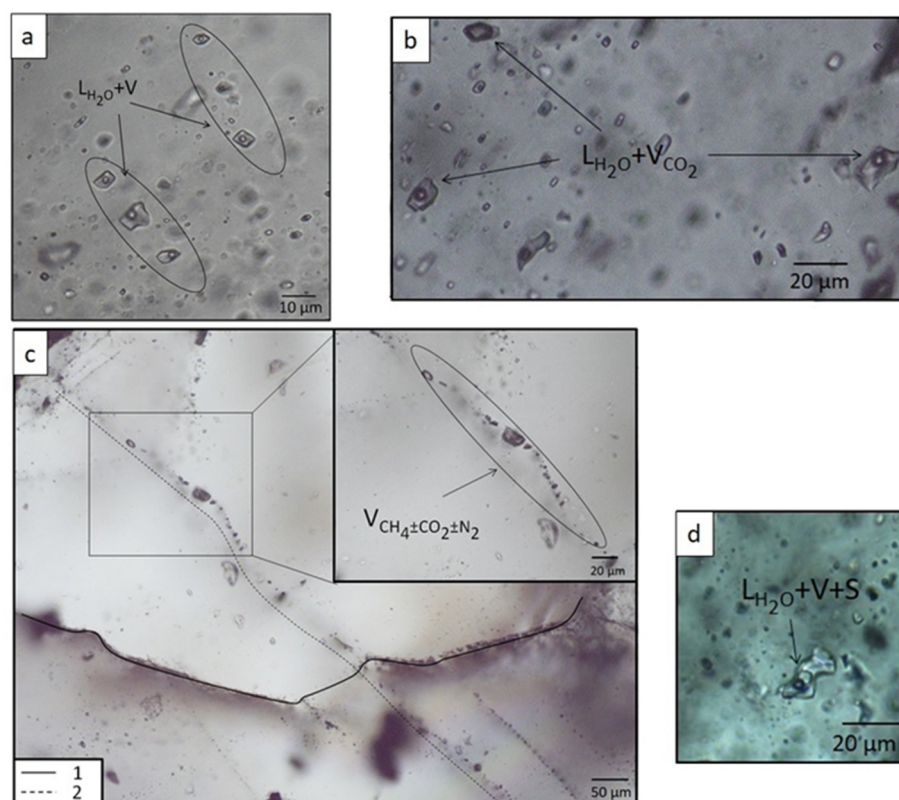


Figure 3. Types of fluid inclusions in quartz from the Blagodatnoye gold-ore deposit: (a)—type A, (b)—type B, (c)—type C (1—grain boundary, 2—secondary FI cutting the grain boundary), (d)—type D.

Among examined 65 quartz plates, no quartz grains with growth zones were found. We used the following criteria to distinguish between FI generations [41,42]. The primary and pseudosecondary generations are inclusions that are either evenly distributed throughout the quartz grain or form groups of 5–10 inclusions outside healed cracks. The inclusions of secondary generations form chains in healed cracks, which cross the borders of quartz grains.

Vein quartz of pre-ore metasomatites contains primary and pseudosecondary vapor-liquid (type A) and aqueous-carbon dioxide (type B) fluid inclusions the size of which is no more than 5–10 μm . The same quartz contains three types of secondary fluid inclusions localized in cracks that cut the borders of quartz grains. The secondary fluid inclusions with the sizes of vacuoles less than 5–7 μm are filled with the vapor-liquid mixture (type A), in which the liquid H_2O phase prevails. The secondary generation inclusions are single-phase essentially vapor-fluid inclusions (type C, $\text{V}_{\text{CH}_4 \pm \text{CO}_2 \pm \text{N}_2}$) and inclusions with salt crystal (type D, $\text{L}_{\text{H}_2\text{O}} + \text{V} + \text{S}$) (Table 1).

In quartz of ore stage all four types of fluid inclusions were trapped (Table 1, Figure 3): type A primary and secondary generations; type B primary and pseudosecondary generations; type C pseudosecondary and secondary generations; type D secondary generations.

In quartz and calcite from quartz-calcite veins of the post-ore stage, primary vapor-liquid inclusions (type A, $\text{L}_{\text{H}_2\text{O}} \gg \text{V}$) are trapped.

Table 1. Summary of fluid inclusion microthermometric data from the Blagodatnoye gold deposit.

Fluid Inclusion Type	Generation of Fluid Inclusions *	T _h Total, °C	Type of Homogenization **	T _m , °C	Aqueous Phase			T _m of CO ₂ ± CH ₄ ± N ₂ , °C	Partial T _h , °C	Type of Homogenization	Pressure, kbar
					T _{eut} , °C	T _m , °C	Salinity, wt.%, NaCl-eq.				
Pre-ore stage. Quartz of pre-ore metasomatites.											
A L _{H2O} + V	P, PS	180–290 (37)	L	-	-31.3 ÷ -30.5 (19)	-3.0 ÷ -10.0 (15)	6–15	-	-	-	-
	S	140–170 (8)	L	-	-22.0 ÷ -26.3 (3)	-1.0 ÷ -3.0 (3)	2–6	-	-	-	-
B L _{H2O} + L _{CO2} ± CH ₄ ± N ₂	P, PS	250–300 (19)	L	-	-33.4 ÷ -39.0 (11)	-5.9 ÷ -7.0 (11)	10–11	-58.1 ÷ -60.3 (9)	-31.8 ÷ +15.1 (9)	L, V	0.2–1.6
C L(V) _{CO2} ± CH ₄ ± N ₂	S	-	-	-	-	-	-	-59.3 ÷ -61.3 (7)	-19.0 ÷ -23.8 (7)	L, V	-
	S	-	-	-	-	-	-	-103.5 ÷ 120.3 (5)	-90.5 ÷ -92.5 (5)	V	-
D L _{H2O} + V + S	S	190–210 (9)	L	170–200 (3)	-49.4 ÷ -56.0 (5)	-21.4 ÷ -20.5 (5)	>30	-	-	-	-
Ore stage. Quartz of gold-sulfide veins.											
A L _{H2O} + V	P, PS	220–350 (68)	L, V	-	-29.3 ÷ -34.2 (28)	-3.9 ÷ -12.0 (27)	8–16.5	-	-	-	-
	S	130–230 (31)	L	-	-18.0 ÷ -21.5 (15)	-0.5 ÷ -2.5 (15)	1–8.5	-	-	-	-
B L _{H2O} + L _{CO2} ± CH ₄ ± N ₂	P, PS	230–280 (39)	L	-	-36.8 ÷ -45.9 (16)	-6.1 ÷ -8.0 (16)	10–12.5	-57.9 ÷ -63.8 (19)	-53.3 ÷ +21.3 (19)	L, V	1.8–2.6
C L(V) _{CO2} ± CH ₄ ± N ₂	P, PS	-	-	-	-	-	-	-59.0 ÷ -61.3 (31)	-37.6 ÷ +19.8 (31)	L, V	-
	PS	-	-	-	-	-	-	-90.1 ÷ -105.1 (17)	-78.5 ÷ -96.6 (17)	L, V	-
D L _{H2O} + V + S	S	150–250 (19)	L	140–190 (15)	-47.2 ÷ -54.3 (11)	-38.1 ÷ -42.1 (11)	>30	-	-	-	-
Post-ore stage. Quartz, calcite filamentous veins.											
A L _{H2O} >>V	P, PS	Quartz									
		110–180 (9)	L	-	-18.5 ÷ -21.0 (5)	-0.5 ÷ -3.0 (6)	1–6	-	-	-	-
B L _{H2O} >>V	P, PS	Calcite									
		120–160 (7)	L	-	-	-	-	-	-	-	-

Note: * P—primary, PS—pseudosecondary, S—secondary. ** L—into the liquid phase, G—into the gas phase. In parentheses—the number of measurements.

4.2. Homogenization Temperatures, Composition, Salinity and Pressure of Fluid

Results of microthermometric studies of fluid inclusions in quartz from the Blagodatnoye deposit are summarized Table 1.

Pre-ore stage. The temperatures of total homogenization of primary and pseudosecondary fluid inclusions in quartz of pre-ore metasomatites are in range of 180–300 °C with homogenization into the liquid phase. The aqueous phase consists of a mixture of chlorides Na and Mg with the salinity of 6–15 wt.%, NaCl eq. These fluids contain CO₂ and probably CH₄, which is suggested from the melting point (−58.1 ÷ −60.3 °C); the temperature of partial homogenization (into liquid/vapor) is in the range between +15.1 to −31.8 °C (Table 1). Quartz of pre-ore metasomatites contains trapped low-temperature (140–170 °C), low-salinity (2–6 wt.%, NaCl-eq.) aqueous (type A), carbon dioxide–methane–nitrogen (type C) and high-salinity (>30 wt.%, type D) fluid inclusions in the form of second-generation inclusions (Table 1). Fluid pressure at this stage of mineral formation ranged 0.2–1.6 kbar.

Ore stage. The temperatures of total homogenization of primary and pseudosecondary inclusions in quartz of gold-bearing associations varied in the range of 220–350 °C with homogenization into both liquid and vapor. The eutectic temperatures suggest that Mg and Na chlorides are present in the water phase of inclusions (Table 1). Fluid salinity is 8–16.5 wt.%, NaCl eq. Among pseudosecondary and secondary generations of inclusions, one can observe constant presence of inclusions with CO₂ (type B) and carbon dioxide–methane–nitrogen (type C), respectively.

In the secondary inclusions with daughter salt crystals (type D, L_{H₂O} + V + S), the fluid with salinity higher than 30 wt.%, NaCl-eq. is trapped, the salinity background of which is determined by Na and Ca chlorides. The temperature of total homogenization varies in the range of 150–250 °C during homogenization into a liquid phase. In the same temperature range, daughter crystals were dissolved almost simultaneously with the vapor bubble disappearance (Table 1). Crystals appeared again with decreasing temperature.

In the secondary vapor–liquid (type A) inclusions, homogenization temperature range was 130–230 °C during homogenization into liquid, the salinity of the fluid was 1–5 wt.%, NaCl-eq. and the composition of fluid was determined by Na chlorides. Fluid pressure during the mineral formation of gold-bearing associations at the Blagodatnoye deposit varied in the range of 1.8–2.6 kbar (Table 1).

Post-ore stage. Homogenization temperatures of primary and pseudosecondary inclusions in quartz and calcite from thread-like quartz–calcite veins were 110–80 °C during homogenization into a liquid phase. Fluid salinity was 1–6 wt.% (NaCl-equiv.).

4.3. Composition of the Gaseous Phase of Fluid Inclusions

The gas component composition of fluids from the Blagodatnoye gold–ore deposit was determined using Raman spectroscopy and gas chromatography–mass spectrometry (GC-MS). Raman spectroscopy analysis showed that individual inclusions in quartz (type B, L_{H₂O} + L(V)CO₂ ± CH₄ ± N₂ and type C, L(V)CO₂ ± CH₄ ± N₂) contain three main components: CO₂, CH₄ and N₂ (Table 2). Water–carbon–dioxide inclusions (type B) are dominated by CO₂ and N₂, and the content of CH₄ is considerably lower. In carbon–dioxide–hydrocarbon inclusions (type C), CH₄ is prevalent and its content amounts to 98.5 mol.% (Table 2), whereas in the inclusions of type B, it is no more than 9.0 mol.%. Partial homogenization in type B and type C fluid inclusions occurs both to the gas and to liquid phase (Table 2). The CO₂/CH₄ ratio in type B inclusions varies in the range of 4.7–94.0, averaging 47.4 (n = 12), whereas in the inclusions of type C, this value varies from 0.01 to 0.2, averaging 0.1 (n = 8) (Table 2).

Table 2. Microthermometric characteristics and composition of the gas phase of individual fluid inclusions in quartz of the Blagodatnoye gold deposit (according to Raman spectroscopy data).

No. *	T _m , °C	T _h , °C	Type ** of Homogenization	Content, mol. %			CO ₂ /CH ₄
				CO ₂	CH ₄	N ₂	
FI type B (L _{H2O} + L(V) _{CO2 ± CH4 ± N2})							
111/59.3/1	−58.1	+8	L	78	2.0	20.0	39.0
111/59.3/2	−57.1	+10	L	76	2.0	22.0	38.0
111/60.8/1	−56.8	+13	L	94	1.0	5.0	93.0
111/60.8/2	−57.3	+19	L	88	2.0	10.0	44.0
111/90.3/1	−59.5	−6.5	L	81.5	1.0	17.5	81.5
111/90.3/2	−61.2	−9.5	L	74.5	2.5	23.0	29.8
111/120.6/1	−60.3	−8.0	L	85	1.5	13.5	56.7
111/129.5/1	−64.0	−9.5	V	52	1.0	47.0	52.0
111/129.5/2	−63.8	−32.5	L	47	1.5	51.5	31.3
33/29.3/1	-	-	-	74.7	0.9	24.4	83.0
33/29.3/2	-	-	-	42.7	9.0	48.3	4.7
33/29.3/3	-	-	-	61.4	4.0	34.6	15.4
FI type C (L(V) _{CO2 ± CH4 ± N2})							
111/76.5/1	-	−90.0	V	8.0	49.0	43.0	0.2
111/90.3/1	-	−82.0	L	10.5	80.0	9.5	0.1
111/120.6/2	−94.5	−79.0	L	10.5	76.0	13.5	0.1
111/120.6/3	-	−78.5	V	0.0	87.5	12.5	-
111/120.6/4	-	−86.5	V	0.5	98.5	1.0	0.01
111/120.6/5	-	−78.5	L	11.0	86.5	2.5	0.1
111/129.5/3	-	−83.0	L	4.5	86.0	13.5	0.05
111/129.5/4	-	−84.0	V	0.5	98.0	1.5	0.01
33/29.3/4	-	-	-	7.7	38.6	53.5	0.2

Note: * hereinafter, the first digit is the N of the well, the second is the depth in meters, and the third is the inclusion number; ** type of homogenization: L—into the liquid phase, V—into the vapor phase.

Gas chromatography–mass spectrometry (GC-MS) analysis showed that fluid inclusions from quartz, arsenopyrite, pyrrhotite and calcite contains water, carbon dioxide and a wide range of oxygen-free and oxygenated hydrocarbons, nitrogenated, sulfonated and halogenated compounds (Table 3, Supplementary Tables S1–S14). Table 3 shows the most representative results and in Figure 4b data of 14 samples are given. The total number of detected compounds in fluids from the Blagodatnoye deposit reaches 209 in sulfides, 168 in quartz and 162 in calcite.

The GC-MS data indicate that water and carbon dioxide are the main components of fluids from the Blagodatnoye deposit. This is suggested from the CO₂/CO₂ + H₂O ratio, which is always below 1, varying in the range of 0.01 to 0.15 both in quartz and in sulfides (Table 3).

Table 3. Content (rel.%) and number (in parentheses) of volatiles extracted by mechanical shock crushing of minerals from the Blagodatnoye deposit (according to GC-MS).

Component	Mineral Association						
	Gold-Bearing (Au = 1–35.5 g/t)				Barren (Au = 0.2–0.8 g/t)		
	Quartz	Quartz	Arseno-Pyrite	Arseno-Pyrite	Quartz	Pyrrhotite	Calcite
	111/90.3	7/96.0	7/96.0	BKS-10	86/107.7	34/105.9	35/178.1
	Aliphatic hydrocarbons						
Paraffins (alkanes)	1.27 (16)	7.48 (21)	2.24 (18)	3.64 (14)	1.04 (12)	0.87 (16)	0.57 (16)
Olefins (alkenes)	0.07 (17)	0.12 (19)	1.08 (20)	0.11 (19)	2.77 (31)	0.96 (27)	0.06 (19)

Table 3. Cont.

Component	Mineral Association						
	Gold-Bearing (Au = 1–35.5 g/t)				Barren (Au = 0.2–0.8 g/t)		
	Quartz	Quartz	Arseno-Pyrite	Arseno-Pyrite	Quartz	Pyrrhotite	Calcite
	111/90.3	7/96.0	7/96.0	BKS-10	86/107.7	34/105.9	35/178.1
Cyclic hydrocarbons							
Cycloalkanes, cycloalkenes, arenes, PAH	0.03 (17)	0.09 (14)	0.44 (24)	0.14 (22)	2.27 (16)	0.68 (28)	0.04 (20)
Oxygenated hydrocarbons							
Alcohols, ethers and esters	0.33 (23)	0.61 (19)	0.24 (11)	2.78 (19)	28.14 (28)	0.71 (27)	1.13 (17)
Aldehydes	0.50 (22)	0.30 (24)	0.33 (22)	1.17 (22)	0.85 (17)	1.08 (26)	0.44 (21)
Ketones	0.29 (21)	0.21 (15)	0.08 (11)	0.13 (18)	1.47 (12)	0.91 (21)	0.08 (19)
Carboxylic acids	0.73 (13)	0.76 (15)	0.96 (13)	0.3 (14)	0.95 (12)	5.71 (21)	0.41 (13)
Heterocyclic compounds							
Dioxanes, furans	<0.01 (6)	0.01 (3)	<0.01 (4)	<0.01 (5)	0.02 (4)	0.025 (7)	<0.01 (6)
Nitrogenated compounds							
N ₂ , ammonia, nitriles	0.85 (19)	1.44 (7)	0.38 (3)	1.21 (19)	0.78 (4)	1.71 (22)	23.28 (18)
Sulfonated compounds							
H ₂ S, SO ₂ , CS ₂ , COS, thiophenes	0.06 (8)	0.08 (8)	2.59 (10)	0.24 (10)	0.46 (5)	3.85 (11)	0.22 (9)
Inorganic compounds							
CO ₂	14.77	2.13	1.53	1.48	0.83	10.3	15.09
H ₂ O	81.08	86.78	90.14	89.52	60.42	73.45	58.67
Ar	<0.01	0.01	<0.01	-	<0.01	<0.01	<0.01
Number of components	165	149	139	165	144	209	162
Halogenated compounds: Cl, F, Br	0.004 (4)	0.004 (2)	0.001 (1)	0.001 (2)	0.06 (3)	0.06 (2)	-
Alkanes/alkenes	17.6	60.8	2.1	33.4	0.4	0.9	10.0
CO ₂ /(CO ₂ + H ₂ O)	0.15	0.02	0.02	0.02	0.01	0.12	0.2
Σ(C ₅ -C ₁₇)/Σ(C ₁ -C ₄)	0.1	0.5	0.31	0.04	14.8	0.14	0.63

Note: The relative concentrations (rel.%) of volatile components in the mixture under study were obtained by normalizing the areas of individual chromatographic peaks to the total area of all peaks.

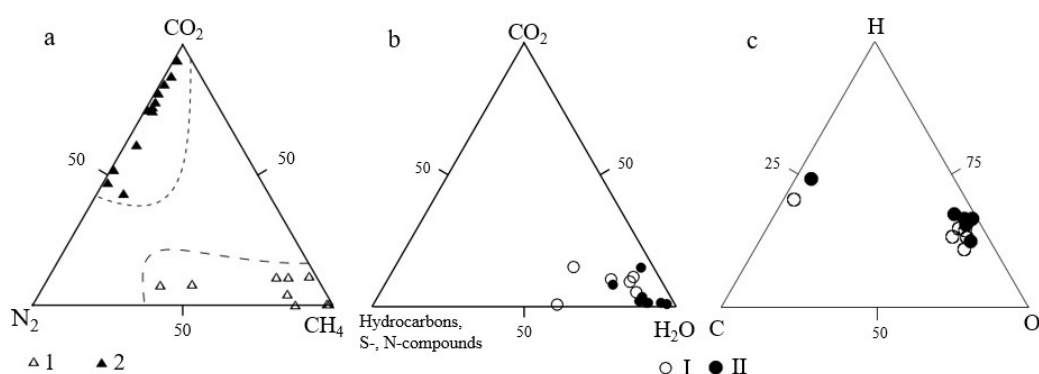


Figure 4. Vapor phase composition of fluid inclusions in minerals of quartz veins from the Blagodatnoye gold deposit (explanations are given in the text): (a) from Raman spectroscopy data. Types of fluid inclusions in quartz: 1—type B, L_{H2O} + L(V)CO₂ ± CH₄ ± N₂; 2—type C, L(V)CO₂ ± CH₄ ± N₂. (b,c) from gas chromatography-mass spectrometry data. Mineral associations: I—gold-bearing, II—barren.

The homologous series of oxygen-free aliphatic hydrocarbons is dominated by methane (CH₄), which accounts for 67.6 to 93.8% in fluid inclusions from minerals of gold-bearing

associations. In fluid inclusions from quartz and sulfides of barren associations, the proportion of CH₄ decreases to 6.3%.

In the group of nitrogenated compounds, molecular nitrogen (N₂) is a prevailing component of the gas phase of fluids both in gold-bearing and barren mineral associations.

A constant component among carboxylic acids is acetic acid, the proportion of which in many fluids of gold-bearing associations averages 22.3% (n = 10) and it is significantly lower in barren associations –8.5% (n = 5).

Sulfonated compounds detected in the gas phase of fluids from quartz and sulfides of gold-bearing and barren associations are dominated by SO₂, the amount of which varies in the range of 42.9% to 98.3%.

Moreover, in the composition of fluids, halogenated compounds such as C₇H₇F, C₄H₄Cl, C₈H₉F, C₆H₁₁BrO, C₁₀H₂₁Cl, C₄H₇ClO were identified, the content of which equals 0.001–0.06 rel.% (Table 3).

4.4. Isotopic Characteristics

Sulfur isotopes ($\delta^{34}\text{S}$) were measured in 27 monofractional microparticles of sulfides, including 5 in pyrrhotite, 4 in pyrite and 18 in arsenopyrite. The isotopic composition of sulfur ranges from 2.6 to 8.9‰ in pyrrhotite, from 9.1 to 11.0‰ in pyrite, and from 6.3 to 20.1‰ in arsenopyrite (Table 4). Most $\delta^{34}\text{S}$ values in arsenopyrite are in a narrower range of 7.7‰ to 12.0‰. Most of $\delta^{34}\text{S}$ values in pyrrhotite are also in the same range (Table 4). The distribution pattern of isotope values of sulfur in sulfides does not change over the studied depth interval (42.6m to 570 m) (Table 4).

Table 4. Sulfur isotopic composition of sulfides from the Blagodatnoye gold deposit.

Sample No.	Mineral	$\delta^{34}\text{S}, \text{‰ CDT}$
34/105.9	pyrrhotite	8.3
53/112.8		2.6
100/216.5		8.9
0166/500		8.7
0166/540		8.6
111/76.5	pyrite	10.1
111/129.5		9.1
B-10		11.0
B-14-b		10.1
7/42.6	arsenopyrite	6.8
7/48.5		9.4
7/61.3		12.0
7/96.0		8.9
87.69.3		6.3
100/221		9.5
100/223		8.7
111/76.5		8.9
111/97.1		11.0
112/191.2		12.0
0166/340		20.1
0166/570		11.2
B-2		7.7
B-3		9.8
B-6		8.9
B-11-a		9.9
B-16		11.6
B17		9.4

Note: The sulfur isotopic composition of sulfides was determined at the Analytical Center for multi-elemental and isotope research SB RAS, Novosibirsk. Analysts: V.N. Reutsky, M.N. Kolbasova.

Carbon isotope composition of carbon-containing compounds in fluid inclusions. Carbon isotopes ($\delta^{13}\text{C}$) were detected in fluid inclusions of gold-bearing and barren quartz (Table 5, Figure 5). The $\delta^{13}\text{C}$ values in fluids of gold-bearing quartz range from -2.8‰ to -12.0‰ . Fluids from barren quartz with gold content less than 0.6 g/t were found to contain a lighter carbon isotope in the range of -3.3‰ to -20.9‰ (Table 5, Figure 5).

Table 5. Carbon isotopic composition ($\delta^{13}\text{C}$) of CO_2 and other carbon-containing compounds in fluid inclusions in quartz of the Blagodatnoye gold ore deposit.

Sample No. *	$\delta^{13}\text{C}_{\text{CO}_2}$, ‰ (VPDB)	Au, g/t
Quartz of gold-bearing associations		
7/48	-10.8	8.6
7/61.3	-2.8	1.6
7/96	-3.0	31.5
100/216.5	-9.8	10.2
100/221	-12.0	1.3
100/223	-10.8	1.6
111/97.1	-4.4	0.8
112/191.2	-3.0	4.9
Quartz of barren associations		
7/55	-10.0	0.6
86/107.7	-17.4	0.2
86/131.8	-3.3	0.2
86/241.4	-4.6	0.3
69/157	-20.9	0.4
34/105.9	-6.4	0.5

Note: * the first digit is the well number, the second is the depth in meters. The isotopic composition of carbon ($\delta^{13}\text{C}$) was determined at the Analytical Center for multi-elemental and isotope research SB RAS, Novosibirsk. Analysts: V.N. Reutsky, M.N. Kolbasova, O. P. Isoch.

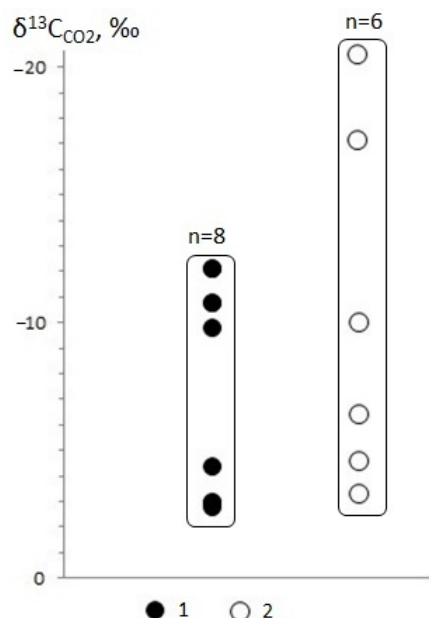


Figure 5. Carbon isotope composition ($\delta^{13}\text{C}_{\text{CO}_2}$, ‰) of carbon-containing compounds of fluid inclusions in gold-bearing (1) and barren (2) quartz from the Blagodatnoye gold deposit.

Isotopes of helium. In fluid inclusions in quartz from ore body No.2 (sample 100/216.5, with gold content 10.2 g/t) ^3He and ^4He isotopes of helium were detected. The contents of ^3He and ^4He are $0.12 \cdot 10^{-12}$ and $0.85 \cdot 10^{-6}\text{ cm}^3/\text{g}$, respectively. The $^3\text{He}/^4\text{He}$ ratio is $0.14 \pm 0.3 \times 10^{-6}$.

Ar–Ar age. Argon–argon dating was used to determine the age of muscovites of schists from the local zones of dynamothermal metamorphism of the Blagodatnoye deposit ore field. The Ar–Ar crystallization age of muscovite is 798.6 ± 6.2 and 735.7 ± 5.9 Ma (Figure 6).

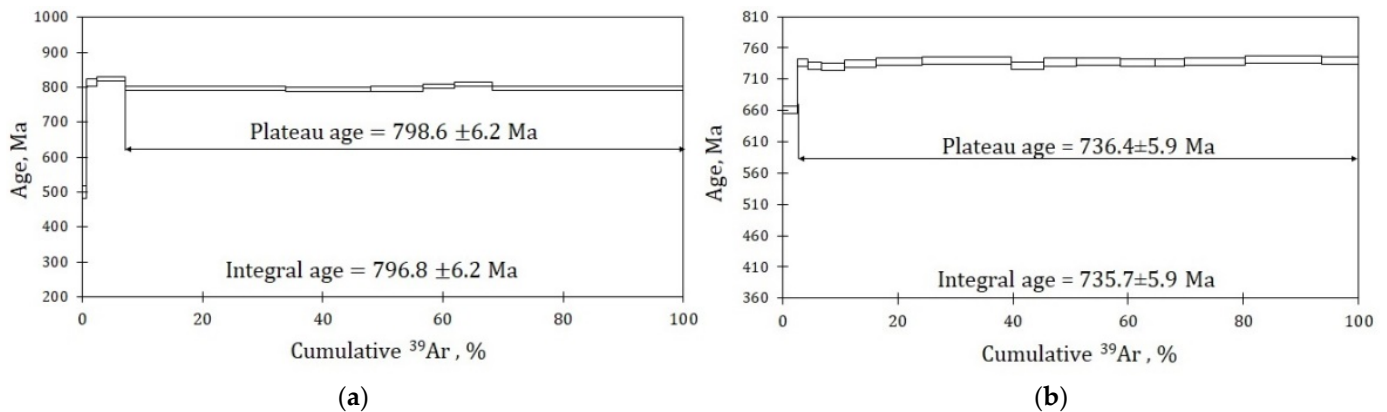


Figure 6. $^{40}\text{Ar}/^{39}\text{Ar}$ age spectra of muscovites from schists of the ore field of the Blagodatnoye deposit: (a)—113–31; (b)—113–54.

5. Discussion

Results of fluid inclusion study in the minerals from the Blagodatnoye gold–ore deposit suggest that the deposit was formed with three types of participation fluid: water–carbon dioxide, carbon dioxide–hydrocarbon and high salinity fluids. The main types are water–carbon dioxide and carbon dioxide–hydrocarbon and, to a lesser degree, high salinity fluid.

The water–carbon dioxide fluid took part in the formation of both gold–bearing and barren quartz–veined zones of the deposit. This is indicated by the presence of gas–liquid (type A, $\text{L}_{\text{H}_2\text{O}} + \text{V}$) and water–carbon dioxide (type B, $\text{L}_{\text{H}_2\text{O}} + \text{L}(\text{V})\text{CO}_2 \pm \text{CH}_4 \pm \text{N}_2$) of primary and pseudosecondary inclusions in quartz (Table 2, Figure 4). This is also suggested from the composition of fluid detected in fluid inclusions in quartz, sulfides and carbonate using GC–MS. The water content in the fluid ranges from 58.7 to 96.4 rel.%, and that of CO_2 —from 0.8 to 15.1 rel.% (Table 3, Supplementary Tables S1–S14). In addition to water and carbon dioxide, the mineral–forming fluid both in gold–bearing and barren veins of the deposit was found to contain a wide range of hydrocarbon compounds (e.g., paraffins, olefins, etc.) and their derivatives as well as nitrogenated, sulfonated and halogenated components. Table 3 demonstrates the most representative results, and Figure 4 shows the results of analysis of 14 samples (Supplementary Tables S1–S14). The total number of detected compounds in one sample reaches 209 (Table 3).

The hydrothermal activity at the Blagodatnoye deposit started from the formation of pre–ore metasomatites consisting of gold–poor ($\text{Au} < 1$ g/t) garnet–bearing quartz–two–mica, quartz–muscovite and their carbonized varieties, often with earlier generations of pyrite, pyrrhotite and vein quartz. The temperature of formation of early quartz–sulfide–parageneses ranged 180 to 300 °C, fluid pressure varied from 0.2 to 1.6 kbar, salinity range was 6–15 wt.%, NaCl–eq. (Table 1).

Raman spectroscopy analysis shows the virtually constant presence of CO_2 in the gas phase of individual inclusions in quartz (Table 2). GC–MS data (Table 3) also indicate the presence of H_2O and CO_2 in the fluid, i.e., the fluid can be attributed to a water–carbon dioxide type. Early thin quartz–sulfide veins were affected by later fluids of carbon dioxide–hydrocarbon and high salinity composition. This suggests by the presence of two generations of secondary fluid inclusions. The first generation is filled with the $\text{CH}_4 \pm \text{N}_2 \pm \text{CO}_2$ mixture, and the second, with the high salinity (>30%) fluid. These generations of secondary inclusions are concentrated in the healed cracks cutting the boundaries of early quartz grains.

The gold-bearing quartz vein bodies of the deposit formed in the temperature range of 220–350 °C, fluid salinity from 8.0 to 16.5 wt.%, NaCl-eq. (Table 1, Figure 7) and fluid pressure from 1.8 to 2.6 kbar. It was revealed, however, in quartz from the ore stage, that homogenization in primary and pseudosecondary fluid inclusions occurred into both liquid and vapor phase, suggesting that the parental fluid was trapped in a heterophase state (Table 1), which was not observed in fluid inclusions in quartz from pre-ore metasomatites. Trapping of fluid in a heterophase (liquid or gaseous) state was, probably, synchronized with strong tectonic movements, which resulted in a series of ore-conducting cracks filled with ore mineralization with gold.

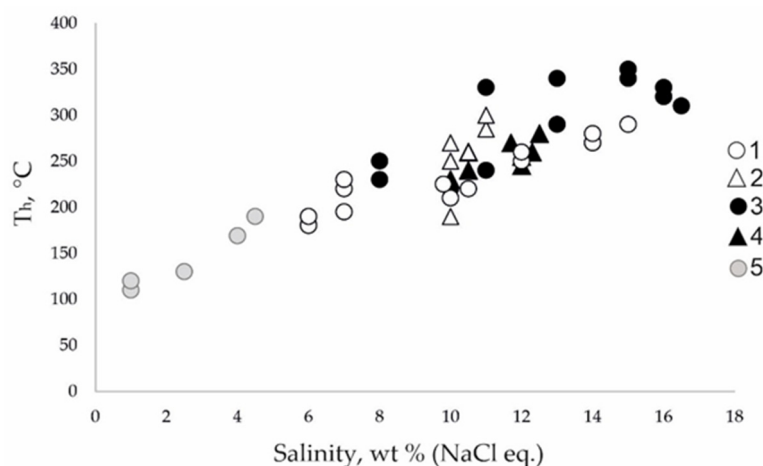


Figure 7. Homogenization temperature (T_h) vs. salinity plot for fluid inclusions in quartz of pre-ore (1—type A, $L_{H_2O} + V$; 2—type B, $L_{H_2O} + L(V)CO_2 \pm CH_4 \pm N_2$), ore (3—type A, $L_{H_2O} + V$, 4—type B, $L_{H_2O} + L(V)CO_2 \pm CH_4 \pm N_2$) and post-ore (5—type A, $L_{H_2O} + V$) stages.

Raman spectroscopic analysis showed that the gas phase of individual fluid inclusions contains various amounts of CO_2 , CH_4 and N_2 (Table 2). The water-carbon dioxide inclusions are dominated by CO_2 , $CO_2/CH_4 > 1$ (Table 2). In the inclusions filled with the $CH_4 \pm N_2 \pm CO_2$ mixture, the proportion of CH_4 increases with $CO_2/CH_4 < 1$. Homogenization in these inclusions occurs to vapor, suggesting a gaseous state of the fluid. Data from [5–9,43,44] show that the CO_2/CH_4 value is an indicator of redox conditions of hydrothermal systems. Based on this fact, the fluid trapped in the inclusions in which $CO_2 > CH_4$ (CO_2/CH_4 value ranges from 15.4 to 93.0, Table 2) is attributed to the oxidized type. In the inclusions filled with the $CH_4 \pm N_2 \pm CO_2$ mixture, the proportion of CH_4 increases, CO_2/CH_4 values range from 0.01 to 0.2 (Table 2) and this fluid is attributed to the reduced type.

The redox properties of the fluids participating in the formation of the Blagodatnoye deposit are indicated by data on the composition of volatile components in inclusions of quartz and sulfides obtained by GC-MS (Table 3). The redox properties of fluids are suggested from the ratio of alkanes to alkenes [45,46]. GC-MS data (Table 3) show that in the fluids of gold-bearing associations of the Blagodatnoye deposit the alkane/alkene value is 28.5, and in barren, it is 3.8, suggesting redox properties of mineral-forming fluids. Thus, gold-bearing fluids were slightly more reduced than the gold-poor ones.

Quartz-veined zones of the deposit were formed mainly by oxidized fluid of water-carbon dioxide composition. Early quartz in these zones was overlain by carbon dioxide-hydrocarbon fluid with reducing properties. The observations of T.V. Poleva and A.M. Sazonov [24] showed that native gold in the studied wells of the Blagodatnoye deposit is typically occurs in the microcracks of quartz. The similar microcracks were healed by $CH_4 \pm N_2 \pm CO_2$ fluid which is a reduced fluid accompanying the segregations of invisible gold. All of this suggests that this fluid was a gold-transporting fluid.

The main argument supporting the conclusions gold was transported by reduced carbon dioxide–hydrocarbon fluid is the composition of fluid extracted from fluid inclusions in native gold from the Sovetskoe deposit. GC-MS analysis showed that the proportion of hydrocarbons in total with S–N–Cl–F–Si–compounds in the composition of gold-bearing fluid reaches 52.0 rel.% [21].

At all depth levels of the occurrence of quartz veinlets and veins of the deposit (from 42 to 680 m), gaseous carbon dioxide–hydrocarbon inclusions were found in quartz, i.e., gaseous fluids functioned at all levels of the hydrothermal system, and were, most likely, coming from deeper horizons and deep long-term sources. A similar pattern was revealed at the Olimpiada giant gold deposit in the depth interval from 4.5 m (well 503) to 817 m (well 510) of ore body No. 4 in the Eastern area of the deposit [19], at the Panimba deposit at the depth up to 692.5 m (well 145) [18], and at the Eldorado gold deposit [20].

Quartz veinlets, veins, lenses and nodules of pre-ore and ore stages of hydrothermal activity are frequently broken by a system of cutting later cracks filled with calcite, white transparent quartz, occasionally with fluorite, which were formed at the post-ore stage. In quartz and calcite of tread-like veinlets only aqueous (liquid–vapor) primary and pseudosecondary inclusions are trapped, the homogenization temperature of which is in the range of 110–180 °C with homogenization to liquid. The salinity of this fluid is no higher than 6 wt.% (NaCl–equiv.) (Table 1, Figure 7). The fluid taking part in the formation of thread-like quartz–calcite veinlets is a water–carbon dioxide type with the predominance of H₂O, CO₂ and nitrogenated compounds (Table 3).

Nitrogenated compounds found in fluid inclusions in quartz, sulfides and calcite from the Blagodatnoye deposit are dominated by molecular nitrogen (N₂). Its fraction ranges from 71.4 to 99.6%, according to GC-MS data. Elevated contents of N₂ (to 53.5 mol.%) were determined in the gas phase of individual inclusions in quartz, using Raman spectroscopy (Table 2). Molecular nitrogen and nitrogenated compounds are constantly present in the gas phase of fluid inclusions in native gold [21]. Nitrogenated, the same as sulfonated and halogenated compounds, may take part in complex formation and transport of gold [47–50].

The presence of molecular nitrogen and nitrogenated compounds in the fluid is most likely related to the chemical reactions between the fluid and ammonium-bearing silicates of host rocks in which nitrogen in the form of NH₄⁺ isomorphically substitutes potassium at the regressive stage of metamorphism [51–53]. The presence of N₂ in the fluid is, probably, related to the decomposition of organic substance of carbon-bearing schists present at the deposit. The most intense decomposition takes place in the zones of maximum hydrothermal–metasomatic processing of host terrigenous rocks in which the role of ammonium nitrogen decreases and N₂ becomes the predominant component [54,55].

Sulfide sulfur of arsenopyrite, the main gold concentrator at the Blagodatnoye deposit [4], is enriched with heavy isotope in a narrow range of variations from 6.3 to 12.0‰ (Table 4). More than 90% values lie even in a narrower range of 7.7 to 12.0‰. The high homogeneity of sulfur is also preserved throughout the depth of occurrence of quartz-veined zones from 42.0 m (well 7) to 570 m (well 0166) (Table 4). Most of δ³⁴S values of pyrite and pyrrhotite are within the same range. The obtained isotope values of sulfur sulfides from the Blagodatnoye deposit ore bodies are considerably heavier than the range of values (δ³⁴S = 0 ± 3, ‰), attributed to magmatic sulfur [56–58]. Figure 8 shows the composition of sulfur isotopes of sulfides of gold deposits on the Yenisei Ridge: Blagodatnoye, Sovetskoye [10], Eldorado [20], Olimpiada [19], Gerfed [17], Panimba [18] and Bogunai [15]. According to the data obtained, the δ³⁴S value varies over a wide range from 0.8 to 21.3‰. Most of the deposits are characterized by the absence of sulfur isotopic homogeneity, which indicates a variety of sulfur sources in the deposits of the Yenisei Ridge and a complex scheme of their interaction.

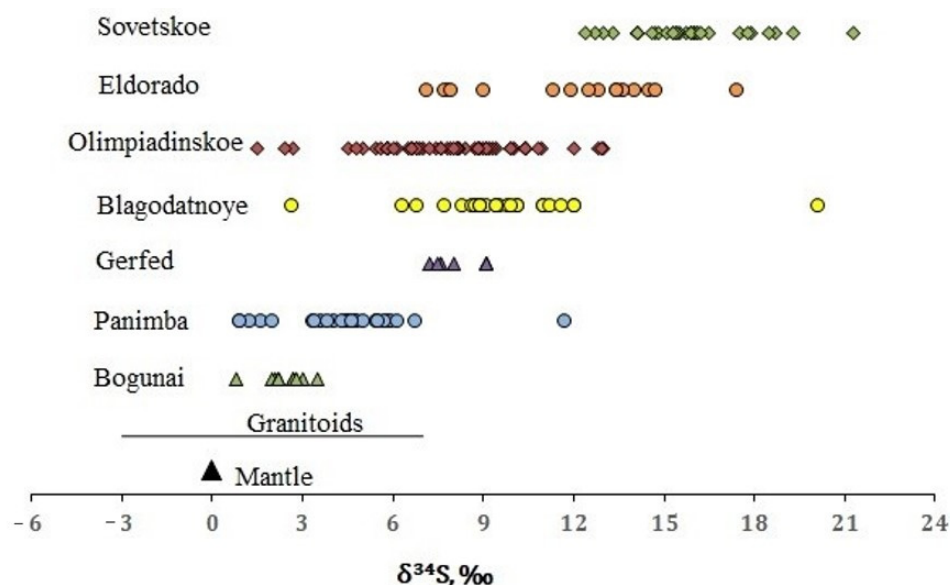


Figure 8. Sulfur isotopic composition of sulfides from gold deposits of the Yenisei Ridge. The sulfur isotopic composition of granitoids is given according to [56].

The obtained data of $\delta^{34}\text{S}$ sulfides from the Blagodatnoye deposit correspond to hydrothermal–sedimentary sulfides of gold–ore deposits in carbon–terrigenous complexes reported in the works of S.G. Kryazhev [14,59]. Sulfur in the ores of the deposit could be obtained by “averaging” the sulfur of host rocks, which suggests its crustal origin [60].

Carbon isotope data show that $\delta^{13}\text{C}$ in early barren fluid varies between -3.3 to -20.9‰ (Table 5, Figure 5). While that of gold-bearing fluid demonstrates a more “heavier” isotope composition (-2.8 to -12.0‰). This confirms that at the ore stage the fluid was more reduced (contained more organic compounds) than the pre-ore barren fluid.

Helium isotopes were detected in fluid inclusions in quartz from ore body No. 2 (sample 100/126.5, Au = 10.2 g/t) at the Blagodatnoye deposit. Helium content in the fluids is ${}^3\text{He} = 0.12 \times 10^{-12}$ and ${}^4\text{He} = 0.85 \times 10^{-6}$, at these parameters the ratio ${}^3\text{He}/{}^4\text{He} = 0.14 \pm 0.3 \times 10^{-6}$. It is shown in [36–38] that the mantle fluid is enriched with ${}^3\text{He}$, and the crustal fluid, with ${}^4\text{He}$. The fraction of mantle helium calculated by the procedure from [39,61] in the fluids from the Blagodatnoye deposit is about 1%. It should be noted that ${}^3\text{He}/{}^4\text{He}$ value of the other deposits of the Yenisei ridge—Sovetskoye, Eldorado, Olimpiada, Gerfed, Panimba and Bogunai—is similar to that of the Blagodatnoye deposit [10,15,17–20]. This fact indicates a crustal fluid source for all these deposits.

Results of isotope–geochemical ($\delta^{34}\text{S}$, $\delta^{13}\text{C}$, ${}^3\text{He}/{}^4\text{He}$) and thermobarochemical studies indicate a crustal origin of the fluids which formed the gold mineralization at the Blagodatnoye deposit.

Isotope (Rb–Sr, Ar–Ar) studies were used to determine the age of the main periods of the formation of the Blagodatnoye deposit [23–26,62,63]. Data of these researchers show that the regional metamorphism of the ore–bearing Riphean Cordaformation occurred in the time interval of 1190–1030 Ma. The age of local dynamothermal metamorphism, which resulted in the schist–forming zones hosting the quartz–veined formations of the deposit, is 826–775 Ma. The age (Ar–Ar method) of crystallization of muscovite from schists of local zones of the ore field of the deposit, determined by us, is 798–735 Ma (Figure 6) and is consistent with the previously determined age (Rb–Sr method) [24]. Thus, the stage of productive sulfide mineralization with gold lasted for about 50–60 Ma [23,26]. Long-term functioning of the hydrothermal system of the Blagodatnoye deposit can be associated with the thermal effect of the mantle plume activity. According to Gertner [64], it probably controlled the mobilization of hydrothermal fluids in the metamorphic formations. The variability of parameters (pressure, temperature, redox) can be associated with unstable environment, reflecting the tectonic activity of the Yenisei ridge.

The host rocks of the deposit are intruded by granitoids of the Tatarka-Ayakhta complex within the period of 880–752 Ma [24,65]. The period of intrusion of granitoids is close to the age of dynamothermal metamorphism. Granites themselves, in the researchers' opinion [66,67], are unlikely to be the sources of gold-bearing fluids but they could be responsible for the more slowly cooling of the ore deposition area and thus support longer-term functioning of hydrothermal solutions. This scenario does not rule out the paragenetic relationship between the post-magmatic solutions of granitoids and high salinity fluids present in the form of secondary inclusions in quartz of quartz-veined zones of the deposit.

6. Conclusions

1. The geological, mineralogical and thermobarochemistry data indicate that the formation of the Blagodatnoye deposit took place with the participation of three types of fluid: water-carbon dioxide (oxidized), carbon dioxide-hydrocarbon (reduced) and, to a lesser degree, high salinity fluid. The deposit was formed in the temperature range of 120–350 °C, pressures 0.2–2.6 kbar and salinity from 0.5 to 30 wt.% (NaCl-equiv.).
2. Mineral-forming fluids contained H₂O, CO₂, hydrocarbons and oxygenated organic compounds, S-, N-, halogenated compounds, which are potentially capable to transport ore elements, including gold.
3. Early barren quartz vein zones of the deposit were formed by oxidized water-carbon dioxide fluids.
4. Later reduced carbon dioxide-hydrocarbon fluids had a key role in the formation of gold-bearing quartz veins when superimposed on the earlier formed quartz. The stage of productive gold-sulfide mineralization at the deposit lasted for about 50–60 Ma.
5. The scales of mineralization depend on the long-term activity of gold-bearing fluids, which is reflected in the degree of saturation of quartz with carbon dioxide-hydrocarbon inclusions.

Supplementary Materials: The following are available online at <https://www.mdpi.com/article/10.3390/min11101090/s1>, Table S1. Results of GC-MS analysis of volatiles extracted by mechanical shock crushing from quartz (Blagodatnoye deposit, Yenisei ridge), Table S2. Results of GC-MS analysis of volatiles extracted by mechanical shock crushing from quartz (Blagodatnoye deposit, Yenisei ridge), Table S3. Results of GC-MS analysis of volatiles extracted by mechanical shock crushing from arsenopyrite (Blagodatnoye deposit, Yenisei ridge), Table S4. Results of GC-MS analysis of volatiles extracted by mechanical shock crushing from arsenopyrite (Blagodatnoye deposit, Yenisei ridge), Table S5. Results of GC-MS analysis of volatiles extracted by mechanical shock crushing from quartz (Blagodatnoye deposit, Yenisei ridge), Table S6. Results of GC-MS analysis of volatiles extracted by mechanical shock crushing from pyrrhotite (Blagodatnoye deposit, Yenisei ridge), Table S7. Results of GC-MS analysis of volatiles extracted by mechanical shock crushing from calcite (Blagodatnoye deposit, Yenisei ridge), Table S8. Results of GC-MS analysis of volatiles extracted by mechanical shock crushing from quartz (Blagodatnoye deposit, Yenisei ridge), Table S9. Results of GC-MS analysis of volatiles extracted by mechanical shock crushing from arsenopyrite (Blagodatnoye deposit, Yenisei ridge), Table S10. Results of GC-MS analysis of volatiles extracted by mechanical shock crushing from pyrite (Blagodatnoye deposit, Yenisei ridge), Table S11. Results of GC-MS analysis of volatiles extracted by mechanical shock crushing from quartz (Blagodatnoye deposit, Yenisei ridge), Table S12. Results of GC-MS analysis of volatiles extracted by mechanical shock crushing from quartz (Blagodatnoye deposit, Yenisei ridge), Table S13. Results of GC-MS analysis of volatiles extracted by mechanical shock crushing from quartz (Blagodatnoye deposit, Yenisei ridge), Table S14. Results of GC-MS analysis of volatiles extracted by mechanical shock crushing from quartz (Blagodatnoye deposit, Yenisei ridge).

Author Contributions: Conceptualization, E.S., N.G. and A.T.; methodology, A.T. and T.B.; investigation, N.G., E.S., M.K., M.R. and M.P.; resources, A.S., S.S. and N.N.; writing—original draft preparation, E.S. and N.G.; writing—review and editing, A.T., T.B., A.S. and S.S. All authors have read and agreed to the published version of the manuscript.

Funding: The work is done on state assignment of IGM SB RAS and was funded by RFBR, project number 19–35–90050.

Data Availability Statement: Data is contained within the article or supplementary material.

Acknowledgments: We sincerely thank four anonymous reviewers whose valuable comments and suggestions helped improve and clarify this manuscript.

Conflicts of Interest: The authors declare no conflict of interest.

References

1. Polus Gold. Available online: <https://polyus.com/en/> (accessed on 15 September 2021).
2. Prokofiev, V.Y.; Bortnikov, N.S.; Garofalo, P. Physicochemical parameters and composition of ore-forming fluids of orogenic gold deposits in Russia. In Proceedings of the XIII International Conference on Thermobarogeochemistry and IV APIFIS Symposium, 22–25 September 2008, IGM RAN: Moscow, Russia; 2008; Volume 2, pp. 188–191.
3. Groves, D.I.; Goldfarb, R.J.; Santosh, M. The conjunction of factors that lead to formation of giant gold provinces and deposits in non-arc settings. *Geosci. Frontiers*. **2016**, *7*, 303–314. [[CrossRef](#)]
4. Sazonov, A.M.; Kirik, S.D.; Silyanov, S.A.; Bayukov, O.A.; Tishin, P.A. Typomorphism of arsenopyrite from the Blagodatnoe and Olimpiada gold deposits (Yenisei ridge). *Mineralogy* **2016**, *3*, 53–70. (In Russian)
5. Bortnikov, N.S.; Prokov'ev, V.Y.; Razdolina, N.V. Origin of the Charmitan gold–quartz deposit (Uzbekistan). *Geol. Ore Depos.* **1996**, *38*, 238–256.
6. Kryazhev, S.G. *Isotope–Geochemical Regime of the Rormation of the Gold Ore Deposit Muruntau*; TsNIGRI: Moscow, Russia, 2002. (In Russian)
7. Safonov, Y.G.; Prokofiev, V.Y. Model of cosedimentation hydrothermal formation of gold–bearing reefs of the Witwatersrand basin. *Geol. Ore Depos.* **2006**, *48*, 475–511. [[CrossRef](#)]
8. Ronde, C.E.J.; Faure, K.; Bray, C.J.; Whitford, D.J. Round Hill shear zone–hosted gold deposit, Macraes Flat, Otago, New Zealand; evidence of a magmatic ore fluid. *Econ. Geol.* **2000**, *95*, 1025–1048.
9. Jia, Y.; Li, X.; Kerrich, R. A fluid inclusion study of Au–bearing quartz vein systems in the Central and North Deborah deposits of the Bendigo gold field, Central Victoria, Australia. *Econ. Geol.* **2000**, *95*, 467–494. [[CrossRef](#)]
10. Tomilenko, A.A.; Gibsher, N.A.; Dublaynsky, Y.V.; Dallai, I. Geochemical and isotopic properties of fluid from gold–bearing and barren quartz veins of the Sovetskoye deposit (Siberia, Russia). *Econ. Geol.* **2010**, *105*, 375–394. [[CrossRef](#)]
11. Dubessy, J.; Poty, B.; Ramboz, C. Advances in C–O–H–N–S fluid geochemistry based on micro–Raman spectrometric analysis of fluid inclusions. *Eur. J. Miner.* **1989**, *1*, 517–534. [[CrossRef](#)]
12. Laverov, N.P.; Prokofiev, V.Y.; Distler, V.V.; Yudovskaya, M.A.; Spiridonov, A.M.; Grebenschikova, V.I.; Matel, N.L. New data on conditions of ore deposition and composition of ore–forming fluids of the Sukhoi Log gold–platinum deposit. *Rep. Acad. Sci.* **2000**, *371*, 88–92.
13. Prokofiev, V.Y.; Naumov, V.B.; Mironova, O.F. Physicochemical parameters and geochemical features of fluids of Precambrian gold deposits. *Geochem. Int.* **2017**, *55*, 1047–1065. [[CrossRef](#)]
14. Kryazhev, S.G. Genetic Models and Criteria for Prediction of Gold Deposits in Carbon–Terrigenous Complexes. DSci. Thesis, TsNIGRI, Moscow, Russia, 2017. (In Russian).
15. Ryabukha, M.A.; Gibsher, N.A.; Tomilenko, A.A.; Bul'bak, T.A.; Khomenko, M.O.; Sazonov, A.M. PTX–parameters of metamorphogene and hydrothermal fluids; isotopy and age of formation of the Bogunai gold deposit, southern Yenisei ridge (Russia). *Russ. Geol. Geophys.* **2015**, *56*, 903–918. [[CrossRef](#)]
16. Khomenko, M.O.; Gibsher, N.A.; Tomilenko, A.A.; Bul'bak, T.A.; Ryabukha, M.A.; Semenova, D.V. Physicochemical parameters and age of the Vasil'kovskoe gold deposit (Northern Kazakhstan). *Russ. Geol. Geophys.* **2016**, *57*, 1728–1749. [[CrossRef](#)]
17. Gibsher, N.A.; Tomilenko, A.A.; Sazonov, A.M.; Ryabukha, M.A.; Timkina, A.L. The Gerfed gold deposit: Fluids and PT–conditions for quartz vein formation (Yenisei Ridge, Russia). *Russ. Geol. Geophys.* **2011**, *52*, 1461–1473. [[CrossRef](#)]
18. Gibsher, N.A.; Ryabukha, M.A.; Tomilenko, A.A.; Sazonov, A.M.; Khomenko, M.O.; Bul'bak, T.A.; Nekrasova, N.A. Metal–bearing fluids and the age of the Panimba gold deposits (Yenisei Ridge, Russia). *Russ. Geol. Geophys.* **2017**, *58*, 1366–1383. [[CrossRef](#)]
19. Gibsher, N.A.; Tomilenko, A.A.; Bul'bak, T.A.; Ryabukha, M.A.; Khomenko, M.O.; Shaparenko, E.O.; Sazonov, A.V.; Sil'yanov, S.A.; Nekrasova, N.A. The Olimpiadinskoe gold deposit (Yenisei ridge): Temperature, pressure, composition of ore–forming fluids, $\delta^{34}\text{S}$ in sulfides, $^3\text{He}/^4\text{He}$ of fluids, Ar–Ar age, and duration of formation. *Russ. Geol. Geophys.* **2019**, *60*, 1043–1059. [[CrossRef](#)]
20. Gibsher, N.A.; Tomilenko, A.A.; Sazonov, A.M.; Bul'bak, T.A.; Khomenko, M.O.; Ryabukha, M.A.; Shaparenko, E.O.; Sil'yanov, S.A.; Nekrasova, N.A. Ore–bearing fluids of the Eldorado gold deposit (Yenisei Ridge, Russia). *Russ. Geol. Geophys.* **2018**, *59*, 983–996. [[CrossRef](#)]
21. Bul'bak, T.A.; Tomilenko, A.A.; Gibsher, N.A.; Sazonov, A.M.; Shaparenko, E.O.; Ryabukha, M.A.; Khomenko, M.O.; Sil'yanov, S.A.; Nekrasova, N.A. Hydrocarbons in fluid inclusions from native gold, pyrite, and quartz of the Sovetskoe deposit (Yenisei ridge, Russia) according to Pyrolysis–Free Gas Chromatography–Mass Spectrometry Data. *Russ. Geol. Geophys.* **2020**, *11*, 1260–1282. [[CrossRef](#)]

22. Vernikovskiy, V.A.; Vernikovskaya, A.E.; Kotov, A.B.; Sal'nikova, E.B.; Kovach, V.P. Neoproterozoic accretionary and collisional events on the western margin of the Siberian craton: New geological and geochronological evidence from the Yenisey ridge. *Tectonophysics* **2003**, *375*, 147–168. [[CrossRef](#)]
23. Sazonov, A.M.; Ananyev, A.A.; Poleva, T.V.; Khokhlov, A.N.; Vlasov, V.S.; Zvyagina, E.A.; Fedorova, A.V.; Tishin, P.A.; Leontiev, S.I. Gold ore metallogeny of the Yenisei ridge: Geological–structural position, structural types of ore fields. Journal of Siberian Federal University. *Eng. Technol.* **2010**, *4*, 371–395.
24. Poleva, T.V.; Sazonov, A.M. *Geology of the Blagodatnoye Gold Deposit in the Yenisei ridge (In Russian)*; ITKOR: Moscow, Russia, 2012; p. 292.
25. Sazonov, A.M.; Gertner, I.F.; Zvyagina, E.A.; Tishin, P.A.; Poleva, T.V.; Leontyev, S.I.; Kolmakov, Y.V.; Krasnova, T.S. Ore-forming conditions of the Blagodat gold deposit in the Riphean metamorphic rocks of the Yenisey ridge according to geochemical and isotopic data. Journal of Siberian Federal University. *Eng. Technol.* **2009**, *2*, 203–220.
26. Sazonov, A.M.; Zvyagina, E.A. Genesis of gold-bearing ores of Blagodatnaya. The state and problems of geological study of the subsoil and the development of the mineral resource base of the Krasnoyarsk Territory. *Krasnoyarsk* **2003**, 247–249. (In Russian)
27. Brown, P.E.; Lamb, W.M. P–V–T properties of fluids in the system $H_2O \pm CO_2 \pm NaCl$: New graphical presentations and implications for fluid inclusion studies. *Geochim. Cosmochim. Acta.* **1989**, *53*, 1209–1231. [[CrossRef](#)]
28. Duan, Z.; Moller, N.; Weare, J.H. A general equation of state for supercritical fluid mixtures and molecular dynamics simulation of mixture PVTX properties. *Geochim. Cosmochim. Acta.* **1996**, *60*, 1209–1216. [[CrossRef](#)]
29. Bakker, R.J. Fluids: New software package to handle microthermometric data and to calculate isochors. *Memoir Geol. Soc.* **2001**, *7*, 23–25.
30. Borisenko, A.S. Studying the salt composition of solutions of gas–liquid inclusions in minerals by the method of cryometry. *Russ. Geol. Geophys.* **1977**, *8*, 16–27. (In Russian)
31. Kirgintsev, A.N.; Trushnikova, L.I.; Lavrentieva, V.G. *Water Solubility of Inorganic Compounds; A Handbook*; Khimiya: Leningrad, Russia, 1972; p. 274. (In Russian)
32. Tomilenko, A.A.; Chepurov, A.I.; Sonin, V.M.; Bul'bak, T.A.; Zhimulev, E.I.; Chepurov, A.A.; Timina, T.Y.; Pokhilenko, N.P. The synthesis of methane and heavier hydrocarbons in the system graphite–iron–serpentine at 2 and 4 GPa and 1200 °C. *High Temp.–High Pressures.* **2015**, *44*, 451–465.
33. Sokol, A.G.; Palyanov, Y.N.; Tomilenko, A.A.; Bulbak, T.A.; Palyanova, G.A. Carbon and nitrogen speciation in nitrogen-rich C–O–H–N fluids at 5.5–7.8 GPa. *Earth Planet. Sci. Lett.* **2017**, *460*, 234–243. [[CrossRef](#)]
34. Pal'yanova, G.A.; Sobolev, E.S.; Reutsky, V.N.; Bortnikov, N.S. Upper Triassic pyritized bivalve mollusks from the Sentachan orogenic gold–antimony deposit, eastern Yakutia: Mineralogy and sulfur isotopic composition. *Geol. Ore Depos.* **2016**, *58*, 513–521. [[CrossRef](#)]
35. Tolstikhin, I.N.; Prasolov, E.M. Methodology for the study of isotopes of noble gases from microswitches in rocks and minerals. Investigation of mineral-forming solutions and melts by inclusions in minerals. *Work. VNIISIMS. Alexandrov.* **1971**, *14*, 86–98.
36. Vetrin, V.R.; Kamenskii, I.L.; Ikorskii, S.V.; Gannibal, M.A. Juvenile helium in Archean enderbites and alkali granites of the Kola Peninsula. *Geochem. Int.* **2003**, *7*, 699–705.
37. Ikorsky, S.V.; Gannibal, M.A.; Avedisyan, A.A. High-temperature impregnation of helium into fluid inclusions in minerals: Experiments with quartz and nepheline. *Dokl. Earth Sci.* **2006**, *411*, 1299–1302. [[CrossRef](#)]
38. Ikorsky, S.V.; Kamensky, I.L.; Avedisyan, A.A. Helium isotopes in contact zones of alkaline intrusions of different size: A case study of the alkaline–ultrabasic Ozernaya Varaka intrusive and Lovozero massif of nepheline syenites (Kola Peninsula). *Dokl. Earth Sci.* **2014**, *459*, 1543–1547. [[CrossRef](#)]
39. Prasolov, E.M.; Sergeev, S.A.; Belitsky, B.V.; Bogomolov, E.S.; Gruzdov, K.A.; Kapitonov, I.N.; Crimean, R.S.; Khalenev, D.O. Isotopic systematics of He, Ar, S, Cu, Ni, Re, Os, Pb, U, Sm, Nd, Rb, Sr, Lu, and Hf in the rocks and ores of the Norilsk deposits. *Geochem. Int.* **2018**, *1*, 50–69. [[CrossRef](#)]
40. Travin, A.V. Thermochronology of Early Paleozoic collisional and subduction–collisional structures of Central Asia. *Russ. Geol. Geophys.* **2016**, *57*, 553–574. [[CrossRef](#)]
41. Ermakov, N.P.; Dolgov, Y.A. *Thermobarogeochemistry*; Nedra: Moscow, Russia, 1979; p. 271. (In Russian)
42. Roedder, E. *Fluid Inclusions in Minerals*; Mir: Moscow, Russia, 1987; Volume 1, p. 558. (In Russian)
43. Eirish, L.V. *Metallogeny of Gold of Priamurye (Amur Region, Russia)*; Vladivostok: Dalnauka, Russia, 2002; p. 194. (In Russian)
44. Robert, F.; Kelly, W.C. Ore-forming fluids in Archean gold-bearing quartz veins at the Sigma Mine, Abitibi green–stone belt, Quebec, Canada. *Econ. Geol.* **1987**, *82*, 1464–1482. [[CrossRef](#)]
45. Norman, D.I.; Blamey, N.; Moore, J.N. Interpreting geothermal processes and fluid sources from fluid inclusion organic compounds and CO_2/N_2 ratios. In Proceedings of the 27th Workshop on Geothermal Reservoir Engineering, Stanford University, Stanford, CA, USA, 28–30 January 2002; pp. 234–243.
46. Blamey, N.J.F. Composition and evolution of crustal, geothermal and hydrothermal fluids interpreted using quantitative fluid inclusion gas analysis. *J. Geochem. Exp.* **2012**, *116–117*, 17–27. [[CrossRef](#)]
47. Marchuk, M.V. Transport of Major Elements and Metals in Reduced Fluids: An Experimental Study. Author's Abstract. Candidate Thesis (Geology and Mineralogy), Institute of the Earth's Crust SB RAS, Irkutsk, Russia, 2008. (In Russian).

48. Bondar, R.A.; Naumko, I.M.; Lyubchak, A.V.; Khokha, Y.V. On the question of the forms of transfer of precious and rare-metal metals to the ore deposition zones of gold deposits. Native Gold, Typomorphism of Mineral Associations, Conditions for the Formation of Deposits, Tasks of Applied Research. *IGEM RAS. Moscow*. **2010**, *1*, 76–78. (In Russian)
49. Lyakhov, Y.V.; Pavlun, N.N. Some Geological and Geochemical Features of Gold Mineralization in Metamorphic and Magmatic Hydrothermal Systems. In *Metallogenic Processes: From Genetic Theories to Prediction and Discovery of New Ore Provinces and Deposits*; IGEM: Moscow, Russia, 2013; p. 144. (In Russian)
50. Williams-Jones, A.E.; Bowell, R.J.; Migdisov, A.A. Gold in solution. *Element* **2009**, *5*, 281–287. [[CrossRef](#)]
51. Bottrell, S.H.; Miller, M.F. The geochemical behaviour of nitrogen compounds during the formation of black shale hosted quartz-vein gold deposits, North Wales. *J. Appl. Geochem.* **1990**, *5*, 289–296. [[CrossRef](#)]
52. Mironova, O.F.; Naumov, V.B.; Salazkin, A.N. Nitrogen in Mineral-Forming Fluids. Gas Chromatography Determination on Fluid Inclusions in Minerals. *Geochem. Int.* **1992**, *7*, 979–991.
53. Yang, Y.; Busigny, V.; Wang, Z.; Xia, Q. The fate of ammonium in phengite at high temperature. *Am. Mineral.* **2017**, *102*, 2244–2253. [[CrossRef](#)]
54. Kol'tsov, A.B. Hydrothermal mineralization in the fields of temperature and pressure gradients. *Geochem. Int.* **2010**, *11*, 1097–1111. [[CrossRef](#)]
55. Zubkov, V.S. Composition and speciation of fluids in the system C–H–N–O–S at P–T conditions of the upper mantle. *Geochem. Int.* **2001**, *39*, 131–145.
56. Ohmoto, H.; Rye, R.O. *Isotopes of Sulfur and Carbon. Geochemistry of Hydrothermal Ore Deposits*; Wiley: New York, NY, USA, 1979; pp. 509–567.
57. Taylor, B.E. Magmatic volatiles: Isotopic variation of C, H, and S. *Rev. Mineral. Geochem.* **1986**, *16*, 185–225.
58. Goldfarb, R.J.; Newberry, R.J.; Pickthorn, W.J.; Gent, C.A. Oxygen, hydrogen, and sulfur isotope studies in the Juneau gold belt, southeastern Alaska: Constraints on the origin of hydrothermal fluids. *Econ. Geol.* **1991**, *86*, 66–80. [[CrossRef](#)]
59. Kryazhev, S.G.; Grinenko, V.A. *The Isotopic Composition and Sources of Sulfur in Gold–Sulphide Deposits of the Yenisei Ridge. Abstracts of the XVIII Symposium on Geochemistry of Isotopes*; GEOKhI RAN: Moscow, Russia, 2007; p. 37. (In Russian)
60. Ohmoto, H. Stable isotope geochemistry of ore deposits. In *Stable Isotopes in High Temperature Geological Processes. Rev. Mineral. Geochem.* **1986**, *16*, 491–560.
61. Khalenev, V.O. He and Ar isotope compositions as a proxy of metallogenic potential in Plutonic Rocks, Norilsk Region. Author's Abstract. Candidate Thesis, Geology and Mineralogy, All-Russian Geological Institute, St. Petersburg, Russia, 2010. (In Russian).
62. Nozhkin, A.D.; Turkina, O.M.; Bobrov, V.A. Radioactive and rare earth elements in metapelites as indicators of composition and evolution of the Precambrian continental crust in the southwestern margin of the Siberian craton. *Dokl. Earth Sci.* **2003**, *391*, 718–722.
63. Nozhkin, A.D. The conditions of placement and geological and geochemical prerequisites for the formation of uranium, gold-uranium, gold and rare metal tools in the Central Metallogenic Belt of the Yenisei Ridge. *Sat. Geology and mineral resources of Siberia. Krasnoyarsk* **2014**, *S3*, 22–27.
64. Gertner, I.; Tishin, P.; Vrublevskii, V.; Sazonov, A.; Zvyagina, E.; Kolmakov, Y. Neoproterozoic alkaline igneous rocks, carbonatites and gold deposits of the Yenisei Ridge, Central Siberia: Evidence of mantle plume activity and late collision shear tectonics associated with orogenic gold mineralization. *Resour. Geol.* **2011**, *61*, 316–343. [[CrossRef](#)]
65. Vernikovskiy, V.A.; Vernikovskaya, A.E. Tectonics and evolution of granitoid magmatism in the Yenisei Ridge. *Russ. Geol. Geophys.* **2006**, *47*, 32–50. (In Russian)
66. Mernagh, T.P.; Bierlein, F.P. Transport and precipitation of gold in Phanerozoic metamorphic terranes from chemical modeling of fluid-rock interaction. *Econ. Geol.* **2008**, *103*, 1613–1640. [[CrossRef](#)]
67. Konstantinov, M.M. Ore-forming systems in the earth's crust. *Izv. Vuzov. Geologiya i Razvedka.* **2009**, *5*, 22–28.